eliminates one choice, leaving $\Gamma_p/\Gamma=0.03$. A reduced width approximately 0.04 of the single-particle limit is implied, and this reduced width compares as favorably with the stripping reduced width as does that for the 898-kev state, in view of the uncertainty of the value of Γ_p for the 429-kev state. Fortunately, the situation is more clearly resolved with respect to the 340-kev state. Since the $N^{15}(p,\gamma)O^{16}$ cross section is so small near 340 kev,[7] it appears that if the correct assignment is $J=1^-$ then this gamma transition is inhibited by isotopic spin selection rules, making the 340-kev state predominantly $T=0$ and the 1028-kev state predominantly $T=1$.

Table I is a summary of the available information for the five excited states in O^{16} studied in the present work. References are given for the values of resonance energies and total widths which were used in the analysis of the scattering data but which were obtained from other work.

ACKNOWLEDGMENTS

The author wishes to express his gratitude to Professor T. Lauritsen, Professor W. A. Fowler, Professor C. C. Lauritsen, Professor R. F. Christy, and Dr. F. S. Mozer for assistance, advice, and helpful discussions during the course of this work.

PHYSICAL REVIEW VOLUME 108, NUMBER 3 NOVEMBER 1, 1957

Study of the $B^{11}+p$ Reactions

G. DEARNALEY, G. A. DISSANAIKE,* A. P. FRENCH,† AND G. LINDSAY JONES‡
Cavendish Laboratory, Cambridge, England

(Received July 15, 1957)

This paper describes a detailed study of the $B^{11}(p,\alpha_0)Be^8$, $B^{11}(p,\alpha_1)Be^{8*}(2\alpha_2)$, and $B^{11}(p,p)$ processes for the region of proton energies spanning the resonances at 0.67 Mev and 1.4 Mev. The measurements include excitation functions and angular distributions, together with the angular correlation between α_1 and α_2 as inferred from the alpha-particle energy spectrum in fixed geometry. The results are analyzed theoretically and are discussed in relation to the findings of other investigators. It is concluded that the complete body of data can be accounted for if the 0.67-Mev resonance (16.57-Mev state of C^{12}) is $(2-)$ and the 1.4-Mev resonance (17.22-Mev state of C^{12}) is $(1-)$, both formed mainly by s-wave protons; this would corroborate the preferred assignments previously suggested. The proton elastic scattering data imply that the ratio Γ_p/Γ is 0.5 for the 0.67-Mev resonance and 0.05 for the 1.4-Mev resonance.

I. INTRODUCTION

THE bombardment of boron-11 with protons, one of the first studied of all nuclear reactions, has presented a curiously intractable problem in the matter of its detailed analysis. The main difficulty is the occurrence of several very broad resonances with an extensive overlap, so that the compound state of C^{12} formed at any given proton energy must normally be thought of as a superposition of states. As a result of this it has been almost impossible to arrive at a clear-cut interpretation of the reaction through studies of only one or two of the possible reaction products. The present paper is the outcome of several investigations (beginning in 1952) carried out with the aim of making our picture of the reaction as complete as possible. None of this work has been previously reported by us, although some of it has been alluded to in papers by other authors.[1–3]

The main concern of this paper is the analysis of the two levels in C^{12} formed at 0.67 and 1.4 Mev in the proton bombardment of B^{11}. The present work had its origin in the discovery,[4] at this laboratory, of the now familiar fact that the resonance formed by protons of 0.163 Mev is able to interfere with another level of opposite parity. The earlier measurements were made solely on the long-range alpha particles (α_0) leading to the ground state of Be^8; to facilitate later discussion we shall enumerate this and all other reactions of interest:

$$B^{11}+p\rightarrow Be^8+\alpha_0, \quad \text{(a)}$$

$$\rightarrow Be^{8*}+\alpha_1, \ (Be^{8*}\rightarrow 2\alpha_2), \quad \text{(b)}$$

$$\rightarrow C^{12}+\gamma_0, \quad \text{(c)}$$

$$\rightarrow C^{12*}+\gamma_1, \quad \text{(d)}$$

$$\rightarrow B^{11}+p. \quad \text{(e)}$$

It was soon discovered, from measurements on the energy dependence of the yield of alpha particles[1,5] and

* Now at the Physical Laboratories, University of Ceylon, Colombo, Ceylon.
† Now at the Physics Department, University of South Carolina, Columbia, South Carolina.
‡ Now at Clifton College, Bristol, England.
[1] Beckman, Huus, and Zupančič, Phys. Rev. **91**, 606 (1953).
[2] H. E. Gove and E. B. Paul, Phys. Rev. **97**, 104 (1955).
[3] Geer, Nelson, and Wolicki, Phys. Rev. **100**, 215 (1955).
[4] Thomson, Cohen, French, and Hutchinson, Proc. Phys. Soc. (London) **A65**, 745 (1952).
[5] G. A. Dissanaike and A. P. French (unpublished).

gamma rays[6,7] up to about 2 Mev that a simple and self-consistent picture was forthcoming. Of the two resonances found above 0.163 Mev, that at 0.67 Mev gave little or no yield of reactions (a) and (c), but was a prolific source of (b) and (d), whereas that at 1.4 Mev exhibited yields of reactions (a) to (d) inclusive. Since the 0.163-Mev resonance was known[4] to be (2+), the interference effects in reaction (a) and the appearance or absence of reactions (a) and (c) could be explained by assuming[1,6,7] that the 0.67-Mev resonance is (2−) and the 1.4-Mev resonance is (1−). This is the conclusion that we ourselves have come to favor, but since this interpretation was first put forward there have been some observations that seemed to call for different assignments of spins and parities. The evidence has been summarized in recent papers[2,3] so we shall not discuss it in detail. The weight of evidence strongly supports the assignment (1−) for the 1.4-Mev resonance, but the status of the 0.67-Mev level has been thrown in doubt in consequence of some measurements on the angular distribution in reaction (d),[8] and to a lesser extent by studies of the $\alpha_1-\alpha_2$ angular correlation in reaction (b).[3] A further complication has been the discovery of some higher resonances for alpha[9] and gamma[2,10] emission, of sufficient strength and width to have an appreciable influence in the region of 1 Mev or even lower.

Our own measurements have been in the following categories:

(i) The excitation functions for reactions (a) and (b).
(ii) The angular distributions of α_0 and α_1 in reactions (a) and (b).
(iii) The angular correlation between α_1 and α_2 in reaction (b).
(iv) The energy and angle dependence of the elastic scattering reaction (e).

There is little need to discuss (i), as the essential features of our results duplicate those of Beckman *et al.*[1] which were obtained independently at the same time. The most important feature is the apparently complete absence of any resonance for reaction (a) at 0.67 Mev, implying that this resonance must belong to the sequence (0−), (1+), (2−), etc. The yield of α_0 rises smoothly through this region of energy, but the existence of a peak yield at about 1.3–1.4 Mev[1,9] seems to demand a resonance of the character (0+), (1−), (2+), etc., at this energy. We shall proceed to discuss our more specific observations (ii), (iii), (iv) in the light of these limitations on the nature of the levels in C^{12}.

[6] T. Huus and R. B. Day, Phys. Rev. **85**, 781 (1952); **91**, 599 (1953).
[7] Cochran, Ryan, Givin, Kern, and Hahn, Phys. Rev. **87**, 672 (1952).
[8] Grant, Flack, Rutherglen, and Deuchars, Proc. Phys. Soc. (London) **A67**, 751 (1954).
[9] E. B. Paul and R. L. Clarke, Phys. Rev. **91**, 463 (1953).
[10] H. E. Gove and E. B. Paul, Phys. Rev. **91**, 463 (1953).

II. ANGULAR DISTRIBUTIONS OF ALPHA PARTICLES

(a) Basis of the Experiments

A study of the angular distribution of α_0 in the reaction $B^{11}(p,\alpha_0)$, leading to Be^8 in its spinless ground state, offers an obvious hope of an easily interpreted result, because the orbital angular momentum of the outgoing alpha particle can take on only one value for a given compound state in C^{12}. Moreover, the absence of the 0.67-Mev resonance with respect to this reaction suggests that in the region between about 0.5 and 1.5 Mev it is mainly the 1.3–1.4 Mev resonance that is concerned. Once definite information has been obtained through this reaction one can hope to learn something of the properties of the 0.67-Mev resonance by studying the angular distribution for $B^{11}(p,\alpha_1)$, in which interference between the two states can take place.

The experiments were conducted by separating out the alpha particles with a magnetic analyzer mounted on a turntable. The particles were detected with a ZnS screen and photomultiplier, and the target was a thin (20 $\mu g/cm^2$) layer of separated B^{11}. All the measurements were made on the Cavendish Laboratory electrostatic generator.

(b) Angular Distributions for α_0

Measurements on α_0 were made for proton energies of 0.64, 0.93, 1.40, and 2.00 Mev, and the results are shown in Fig. 1. Also shown on the figure are the points obtained by Paul and Clarke[11] at 1.39 Mev, with a suitable normalization for comparison with our 1.4-Mev measurements. The most obvious features of these angular distributions are that the intensity falls nearly to zero at 0° and 180°, and that the curves are strongly skewed about 90°, showing interference between states of opposite parity.

At first sight the very large variation of intensity with angle seems to be evidence against taking the 1.4-Mev resonance to be (1−), since one might expect the dominant formation of the state by *s*-wave protons to lead to a nearly isotropic angular distribution. The detailed analysis shows, however, that an admixture of *d*-wave changes the theoretical curve drastically. If we assume first of all that a pure (1−) compound state is

TABLE I. Amplitudes of the 2.0-Mev resonance (*b*) and the 2.6-Mev resonance (*c*) relative to the 1.4-Mev resonance (*a*) at various proton energies.

E_p (Mev)	b/a	c/a
0.3	0.13	0.25
0.7	0.12	0.22
0.9	0.11	0.20
1.1	0.11	0.19
1.4	0.15	0.20
2.0	1.85	0.61

[11] E. B. Paul and R. L. Clarke (private communication of results mentioned in reference 9).

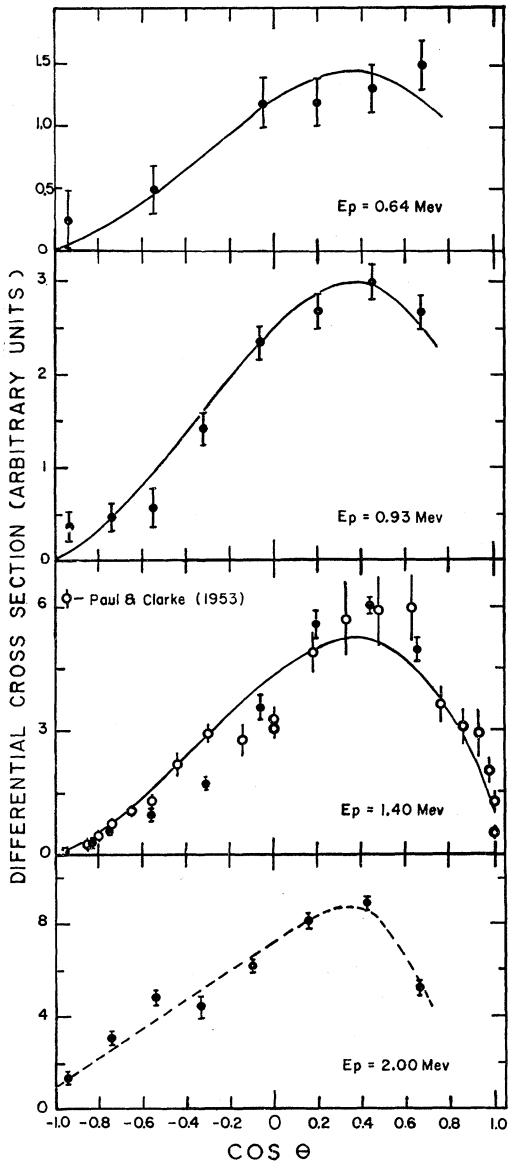

FIG. 1. The angular distribution of the long-range α_0 particles observed for proton energies E_p equal to 0.64, 0.93, 1.4, and 2.0 Mev, respectively. The results of Paul and Clarke at $E_p=1.39$ Mev are also included (after suitable normalization) in the third graph. The smooth curves drawn in the first three graphs represent a theoretical distribution assuming the interference between a (1−) state at 1.4 Mev and a (2+) state at 2.6 Mev. The experimental points for $E_p=2.0$ Mev are fitted empirically by a broken curve.

involved, and that the d-wave contribution to formation of the state is given in amplitude and phase by (A,α), the angular distribution is

$$I(\theta)=[1+\sqrt{2}A\cos\alpha+(\tfrac{1}{2}+\tfrac{3}{2}f)A^2]-\cos^2\theta[3\sqrt{2}A\cos\alpha-(\tfrac{3}{2}-\tfrac{3}{2}f)A^2],$$

where f is ratio of probabilities of having the reaction take place from the spin channels 2 and 1, respectively, in the initial state. Since the final state consists of two spinless particles, there is no ambiguity about the mode of decay.

If we suppose that the intensity for $\theta=0$ or π is *exactly* zero, we obtain the condition

$$A^2-\sqrt{2}A\cos\alpha+\tfrac{1}{2}=0, \text{ independent of } f.$$

The angular distribution then automatically has the form $\sin^2\theta$ for all f, and for all A allowed by the above condition. It will emerge that this simple particular form comes very close to describing the experimental results, but first we must consider the important modifications caused by interference with a compound state (or states) of even parity. The measurements of Paul and Clarke[9] suggest that two such states may exist, *viz.*, a resonance at 2.0 Mev of width about 0.15 Mev and character (0+), and a resonance at 2.6 Mev of width about 0.3 Mev and character (2+). Taking the peak yield of the 1.4-Mev resonance as 1.0, the relative yields of the other resonances become about 1.4 and 2.6 respectively. Let us label the 1.4, 2.0 and 2.6-Mev resonances as a, b, and c respectively. Then Table I shows the amplitudes of b and c relative to a at various proton energies, assuming the relative variations of intensity to be given simply by the Breit-Wigner resonance denominators.

It is interesting to observe that below 1.4 Mev the relative amplitudes are almost constant, and that the 2.6-Mev state has an amplitude about twice as great (and hence an intensity about four times as great) as the 2.0-Mev state. Since the character of the interference effects will be governed largely by the parity, and since the 2.6-Mev resonance is clearly more important than the 2.0-Mev resonance in the greater part of the energy region studied by us, we consider the interference effects due to a single state of character (2+).

If one assumes the (2+) state to be formed by p-wave protons only (for simplicity) and the contribution to its formation relative to that of the (1−) state at some energy to be given in amplitude and phase by (C,γ), the angular distribution becomes:

$$\begin{aligned}I(\theta)\sim{}&1.5+2.12A\cos\alpha+0.75A^2(1+3f_1)+1.25C^2(1+3f_2)\\&+\cos\theta[9.76(1-0.6f_1^{\frac{1}{2}}f_2^{\frac{1}{2}})AC\cos(\alpha-\gamma)+5.48C\cos\gamma]\\&-\cos^2\theta[6.36A\cos\alpha-2.25A^2(1-f_1)-3.75C^2(1-f_2)]\\&-\cos^3\theta[17.42(1-0.33f_1^{\frac{1}{2}}f_2^{\frac{1}{2}})AC\cos(\alpha-\gamma)],\end{aligned}$$

where (A,α) is as before, and the f values again refer to the relative contributions from channel spins 2 and 1 in formation of the compound states, f_1 corresponding here to the (1−) state and f_2 to the (2+) state. We have used this expression to find a theoretical curve to fit the distribution at 1.4 Mev, since at higher proton

TABLE II. Angular distributions for α_1.

E_p (Mev)	$f(\theta)$
0.64	$1+0.1\cos\theta$
0.93	$1+0.08\cos\theta$
1.4	$1+0.1\cos\theta-0.35\cos^2\theta$

energies the ratio b/a (see Table I) tends to increase and would require the consideration of interference due to the resonant state at 2.0 Mev as well. With $C=0.25$, $A^2=\frac{1}{4}$, $\cos\alpha=1$, $\cos\gamma=1$, and f_1, f_2 negligibly small, we obtain a satisfactory fit to the experimental points at $E_p=1.4$ Mev, as seen in Fig. 1. The agreement is not much improved by considering nonzero values for f_1 and f_2 or by changing the other parameters. It is worthy of note also that this theoretical curve agrees reasonably well with the distributions at the proton energies 0.64 and 0.93 Mev shown in Fig. 1, though the distribution at $E_p=2.0$ Mev drops more sharply for θ approaching zero. Considering the data in Table I on the relative amplitudes of the states involved, these findings are not surprising, and lend support to the view that for proton energies up to about 1.4 Mev the (1−) state at 1.4 Mev is influenced mainly by a state (2+) at 2.6 Mev.[12]

(c) Angular Distributions for α_1

In order to obtain some idea of the angular distributions of the α_1 particles, a study was made of the integrated alpha-particle spectrum as a function of angle for various proton energies. The spectrum observed at a given angle consisted of the α_1 group plus the continuum of α_2, and in order to resolve the spectrum we made use of the assumption [see Sec. III (a)] that the total yield of particles above 2.5 Mev represents all the α_1 particles plus half of the α_2 spectrum. However, the α_2 particles detected at an angle θ in the center-of-mass system would correspond to α_1 particles emitted in a finite cone of angles in the opposite direction. This effect would therefore render the method quite insensitive to odd powers of $\cos\theta$ in the distribution but would not affect the even powers.

The distribution patterns $f(\theta)$ as observed in the center-of-mass system for different energies E_p are shown in Table II. The absence of a $\cos^2\theta$ term in the distributions at 0.64 and 0.93 Mev shows that the lower resonance at 0.67 Mev must be formed chiefly by s-waves, and in fact if a (2−) state is assumed, it can be inferred that the d-wave contribution to its formation must be less than 10%. About half the $\cos\theta$ term in the observed distribution might arise as a systematic error due to the procedure mentioned above for evaluating the α_1 yield, *viz.*, the division of the α_2 spectrum at 2.5 Mev for all angles. A study of the excitation function for α_1 shows that the ratio of the amplitude contributions of the resonances at 0.67 and 1.4 Mev respectively varies greatly over the energy region studied, being about 3.3 at 0.67 Mev, 1.7 at 0.9 Mev and 0.42 at 1.4 Mev. Thus, if there were "opposite-parity" interference between the resonant states the $\cos\theta$ term in the distribution would be radically changed as the proton energy was varied. However, the insensitivity of the method of study to odd powers of $\cos\theta$ allows no conclusive deductions from this measurement about the parities of the states. At $E_p=1.4$ Mev the $\cos^2\theta$ term in the distribution can be explained, qualitatively, by considering an admixture of d-wave protons in forming the state at 1.4 Mev, assumed to be (1−), with values of (A,α) as obtained from the (p,α_0) angular distributions [see Sec. II (b)]. The α_1 excitation curves of Paul and Clarke,[11] however, indicate that the influence of higher states, chiefly the (2+) at 2.6 Mev, might be appreciable at this energy, though in a less clear-cut manner than for the (p,α_0) reaction; it has not been considered worthwhile to study such influence in any detail.

III. $\alpha_1-\alpha_2$ ANGULAR CORRELATION

(a) Principle of the Method

The $\alpha_1-\alpha_2$ angular correlation was investigated with fixed geometry by studying the energy spectrum of the continuum of alpha particles formed in the breakup of the excited Be^8 nuclei. The observed energy distribution can be related to the angular-correlation function by a consideration of the dynamics of the process.

We consider the following stages: firstly, the motion of the compound nucleus with velocity $\mathbf{v}_1$ in the direction of the incident protons; secondly, the breakup of the compound nucleus, with the excited Be^8 nucleus recoiling with velocity $\mathbf{v}_2$ in a direction opposite to the α_1 particle; and finally, the breakup of this excited Be^8 nucleus, with the final (observed) particle α_2 emitted with velocity $\mathbf{v}_3$ and at an angle ϕ relative to the direction of $\mathbf{v}_2$. Figure 2 represents the diagram of the velocities involved in the reaction. If the final particles

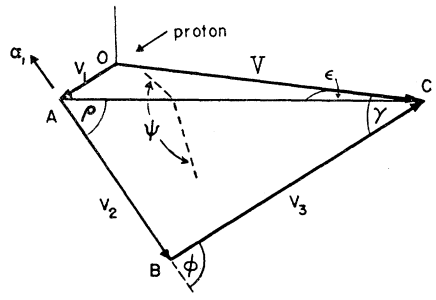

FIG. 2. Velocity diagram for the reaction $B^{11}(p,\alpha_1)Be^{8*}\rightarrow 2\alpha_2$. V is the resultant velocity of the α_2 particles observed at 90° to the direction of the incident proton beam.

[12] A (2+) assignment to the 1.4-Mev state formed by an admixture of p- and f-wave protons gives a distribution approaching a $\sin^2\theta$ type if the contribution to the formation via channel spin 1 is negligible compared to that via channel spin 2. However, the strong interference effects cannot then be explained assuming even parities for the broad resonances beyond 1.4 Mev.

α_2 are detected at right angles to the direction of the incident proton, the resultant velocity $\mathbf{V}$ will be normal to $\mathbf{v}_1$.

The number of α_2 particles reaching the detector can be determined in terms of the velocities and the angles indicated in Fig. 2; ψ is the angle between the planes $(\mathbf{v}_1,\mathbf{V})$ and $(\mathbf{v}_2,\mathbf{v}_3)$. If $\delta\omega$ is the solid angle subtended by the detector at 0, the effective solid angle available to particles from this second breakup will be defined by the intersection of a cone of solid angle $\delta\omega$ and apex 0 with a sphere of radius v_3 and center B. Assuming $\delta\omega$ to be small and the section of the sphere cut off by the cone to be plane, the effective solid angle available to particles in the third stage of the process is thus equal to $V^2\delta\omega/v_3^2\cos\gamma$. If N is the number of processes per unit solid angle in the first breakup (assumed isotropic) and $f(\phi)$ the angular distribution of α_2 with respect to the α_1 particle, then the number dn of α_2 particles reaching the detector is given by

$$dn=N\int_{\psi=0}^{2\pi}\sin\rho d\rho d\psi V^2\delta\omega f(\phi)\Big/ v_3^2\cos\gamma. \qquad (1)$$

For fixed values of v_2, v_3, and ϕ, V is independent of ψ. $\cos\gamma$, however, depends on ψ and, from Fig. 2, may be shown equal to $a-b\cos\psi$, where $a=\cos\epsilon\cos(\phi-\rho)$ and $b=\sin\epsilon\sin(\phi-\rho)$. Substituting for $\cos\gamma$ in Eq. (1) and assuming $b^2<a^2$, we have by integration

$$dn=2\pi N\delta\omega f(\phi)V^2\sin\rho d\rho/(a^2-b^2)^{\frac{1}{2}}. \qquad (2)$$

For $b^2>a^2$ it is clear that there will be a ψ for which $\cos\gamma=0$, i.e., $\mathbf{v}_3$ will be at right angles to $\mathbf{V}$, and in such a case the assumption made earlier that the section of the sphere cut by the narrow cone at C is effectively plane is no longer valid; the curvature of the section has to be considered. For this special case the area of intersection was determined by an actual optical experiment which simulated the conditions of the problem (see appendix). For the greater part of the region, however, $b^2<a^2$ and Eq. (2) is valid.

The values of a and b in Eq. (2) can be obtained by geometry from Fig. 2 in terms of the velocities v_1, v_2, v_3, and V, and therefore in terms of the corresponding energies E_1, E_2, E_3, and E released to the final particle at each stage of the reaction. Equation (2) then reduces to

$$dn=\pi N\delta\omega f(\phi)dE/(E_2E_3)^{\frac{1}{2}}G(E), \qquad (3)$$

where $G(E)=(1+E_1/E)[1-4E_1E_3/(E_1+E-E_2+E_3)^2]^{\frac{1}{2}}$ and $E=E_2+E_3+2(E_2E_3)^{\frac{1}{2}}\cos\phi-E_1$.

If n_0 is the number of α_1 particles received by the detector, then, by considering the fact that there are two α_2's emitted in the breakup of the emitted Be^8 nucleus, it is easily shown that $2n_0=N\delta\omega$ for the case, as in our experiment, where the energy E_1 is much less than the energy of the α_1 particle. Introducing this value of n_0 in Eq. (3) and defining the energy distribution function $g(E)\equiv dn/dE$, we have

$$g(E)=2\pi n_0 f(\phi)/(E_2E_3)^{\frac{1}{2}}G(E). \qquad (4)$$

Thus, the energy distribution function $g(E)$ is related to the angular distribution function $f(\phi)$, and for $E_1=0$, corresponding to a two-stage process, reflects the angular distribution exactly.

The value of $g(E)$ for a particular energy E of the final particles is given by the above equation for a given set of values of E_2 and E_3. The values of E_2, E_3 depend on the values of Q_1 and Q_2, the energy releases in the first and second breakup processes respectively, and therefore on the shape and width of the excited Be^8 state at 2.9 Mev. In the experiment, we assumed for the level a width $\Gamma=1.2$ Mev[1] and a simple resonance shape, so that the factor $1/\{[(Q_2-2.9)/(\frac{1}{2}\Gamma)]^2+1\}$ would determine the distribution of Q_1 and Q_2 and hence also the shape of the α_1 peak. For convenience, n_0 was defined equal to this factor with a value equal to 1 at $Q_2=2.9$ Mev. The numerical evaluation of the energy distribution corresponding to a given pattern $f(\phi)$ could then be carried out. For a particular E of the final (observed) particle, we obtain the contributions to the $g(E)$'s due to each set of E_2, E_3 using Eq. (4), with $\sum g(E)$ giving the ordinate of the calculated energy distribution of the α_2 continuum for that E. The α_1 group is superposed on this continuum, the ordinate at any E being easily determined from the value of n_0 as given by the resonance factor above. The calculated distribution of the continuum plus α_1 group so obtained could then be compared with the observed energy distribution.

The effect on the $g(E)$'s of changing the value of E_p, the incident proton energy, can be readily inferred for $G(E)\simeq 1$ by differentiating Eq. (4) partially with respect to E_1 (and therefore E_p). Thus, for the greater part of the region covered by values of E_2, E_3, and E [for which $G(E)\simeq 1$], we may obtain the change in the $g(E)$'s without a new set of numerical calculations.

The numerical calculations above were first carried out for simple normalized patterns $f(\phi)=1/4\pi$ and $f(\phi)=(3/8\pi)\sin^2\phi$. With the $g(E)$'s calculated for these patterns the energy distributions corresponding to other $f(\phi)$ involving $\cos^2\phi$ or $\sin^2\phi$ terms could be easily deduced.

(b) Results and Interpretation

The experimental energy distribution of the α_2 continuum plus the α_1 group at 90° to an incident proton beam of energy $E_p=0.53$ Mev is shown in Fig. 3. The distribution was studied with a thick target (~90 kev) of boric acid using a 60° focusing magnetic analyzer and a ZnS screen and photomultiplier as detector. The following factors influencing the detection of the particles, especially at the lower energies, were considered and corrected for: (i) the loss in efficiency of the detector, (ii) the spread in energy of the particles

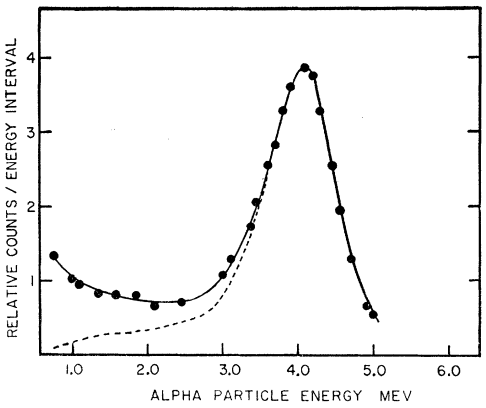

FIG. 3. The experimental energy distribution of the short-range α_1 and the continuum of α_2 particles for $E_p=0.53$ observed at 90° using a thick target (~90 kev) of boric acid. The dotted curve shows the yield (uncorrected) of the alpha particles at the lower energies as actually measured by the magnet analyzer and detector assembly.

accepted by the analyzer, (iii) the loss in number of He^{++} ions due to charge exchange in the target material.[13] The magnitude of the correction applied to the distribution at the lower energies due to these factors may be judged from the dotted curve in the figure which represents the actually observed (uncorrected) yield of the alpha particles at various energies. We cannot therefore place too much reliance on the low-energy region of the distribution, but the region above 2 Mev is considered reliable to about 2%. The shape of the experimental distribution for other values of the proton energy from 0.25 to 1.4 Mev did not appear to be very different from that in Fig. 3.

In the interpretation of this energy distribution we are guided by two important facts arising out of the theory outlined in the previous section. Firstly, the energy distribution function $g(E)$ simulates the angular distribution function $f(\phi)$ for $E\gg E_1$, i.e., for E above about 2.0 Mev; secondly, as much as half the total area under the alpha spectrum above 2.5 Mev must be due to the continuum. Also it is possible to estimate the ratio of the minimum to the (probable) maximum of this continuum, the maximum occurring at about 4-Mev energy. These considerations suggest that $f(\phi)$ should have a minimum value for $\phi\simeq\pi/2$, with a maximum for ϕ near 0 or π.

We have assumed for simplicity that the formation of the compound state of C^{12} at 0.67 Mev takes place with s-wave protons only, as indicated by the results from the (p,α_1) angular distributions [Sec. II (c)], and from the elastic scattering of protons (Sec. IV). The breakup of C^{12} is therefore isotropic in the center-of-mass system, and it is sufficient to consider the theory for a two-stage process only. The state of the compound nucleus may therefore be either (2−) or (1−), the α_1 particle may be emitted as p-wave or as a mixture of p- and f-waves, and the α_2 particle emitted as d-wave only on the assumption that the Be^{8*} state is (2+). With these conditions, we have for a compound state (2−):

$$f_1(\phi)\sim(1-\cos^2\phi)+B_1\cos\beta_1(1-6\cos^2\phi+5\cos^4\phi)+\tfrac{1}{4}B_1^2(1+14\cos^2\phi-15\cos^4\phi), \quad (5)$$

where B_1, β_1 are the amplitude and phase respectively of the outgoing f-wave relative to the outgoing p-wave α_1-particles. For a state (1−):

$$f_2(\phi)\sim2(1+3\cos^2\phi)-2(6)^{\frac{1}{2}}B_2\times\cos\beta_2(1-12\cos^2\phi+15\cos^4\phi)+3B_2^2(1-2\cos^2\phi+5\cos^4\phi). \quad (6)$$

If we assume the outgoing α_1-particle is only p-wave, the distributions above simplify out after normalization into

$$f_1(\phi)=(3/8\pi)\sin^2\phi,$$
$$f_2(\phi)=(1/8\pi)(1+3\cos^2\phi).$$

The theoretical energy distributions for the continuum and the total alpha particles corresponding to these simplified patterns and for the isotropic case $f(\phi)=1/4\pi$ are plotted in Figs. 4(a), (b), and (c) respectively. As is expected, the energy distributions for the continuum simulate the form of the patterns assumed, but none of them conform to the experimental points (represented as circles), since we place great reliance on the accuracy of the experimental distribution at the higher energy region. We next consider the f-wave contributions of the outgoing α_1 particles as well. Since the observed spectrum corresponds to a proton energy E_p of 0.53 Mev, we should expect, from previous evidence, that the compound state be (2−), and the pattern should be, as in Eq. (5), of the form $p+qx-rx^2$ with $p+q=r$ (and $x=\cos\phi$). By using the estimated ratio of the maximum to minimum height of the continuum as deduced from the experimental spectrum, we find indeed that a satisfactory fit may be obtained for $q/p=9$ and $r/p=10$ with a possible variation on these values of about 5%. The energy distribution corresponding to the pattern $f(\phi)=(1/8\pi)\times[1+9\cos^2\phi-10\cos^4\phi]$ is plotted in Fig. 4 (d). The agreement with experiment is good considering, first, that the thick target would tend to broaden out the α_1 group, and second, that the measurements below about 2 Mev would be likely to give unreliable values because of the very large corrections that have to be made for the loss of particles. This pattern gives values of B_1 and β_1 of Eq. (5) as satisfying the equation $B_1^2-12B_1\cos\beta_1-8=0$, so that for example, if $\cos\beta_1=-1$, $B_1\simeq0.6$.

The pattern $f_2(\phi)$ of Eq. (6), corresponding to a compound state (1−) with both p- and f-wave α_1 particles emitted, cannot be fitted satisfactorily with the experimental curve for any values of B_2 and β_2, the closest approach to a fit being obtained with B_2 negligible, corresponding to the simple pattern $1+3\cos^2\phi$

[13] G. A. Dissanaike, Phil. Mag. 44, 1051 (1953).

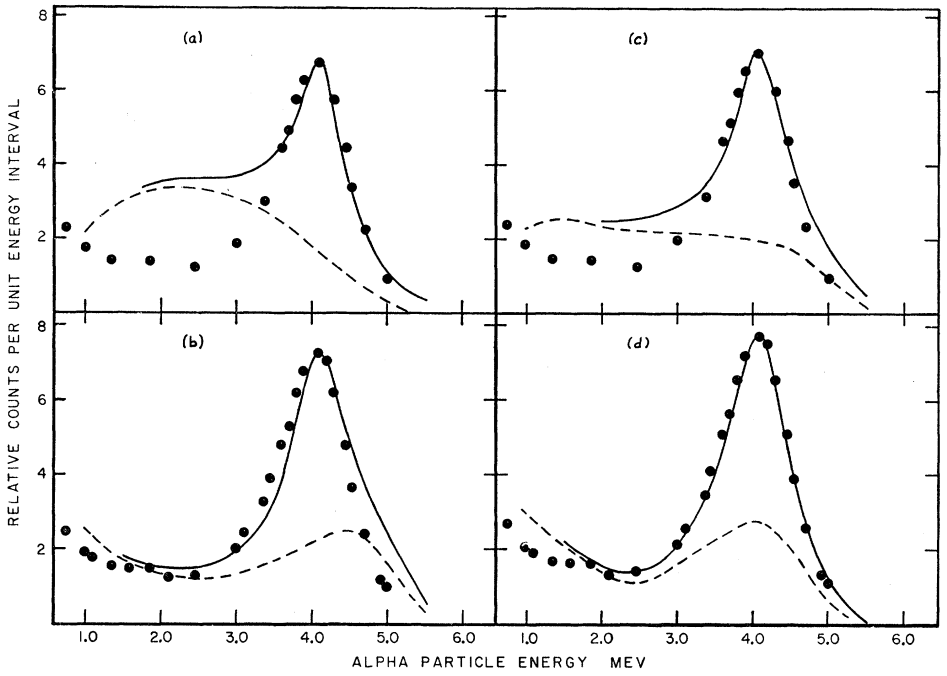

FIG. 4. The theoretical energy distributions for the α_2 continuum (broken curves) and for the total alpha particles (smooth curves) calculated for various angular distribution patterns $f(\phi)$ at $E_p=0.47$ Mev. The experimental values of the alpha-particle spectrum at 90° are represented by circles. The patterns considered are (a) $f(\phi)=(1/8\pi)\times\sin^2\phi$, (b) $f(\phi)=(3/8\pi)\times[1+3\cos^2\phi]$, (c) $f(\phi)=1/4\pi$, and (d) $f(\phi)=(1/8\pi)\times[1+9\cos^2\phi-10\cos^4\phi]$. A value of $E_p=0.47$ Mev is used for the theoretical distributions to make allowance for the energy loss of the incident protons in the thick target (~90 kev) inclined at 45° to the proton beam direction.

already plotted in Fig. 4(b). The contribution due to the 1.4-Mev resonance (about 8% of the total intensity at 0.5 Mev) has not been taken into account in the above considerations. Since the work on the (p,α_1) distributions (Sec. II) gives no obvious indication that the two levels are of opposite parity, and since the shape of the energy distribution of the alpha particles has not shown any significant change over the range of proton energies studied, it is assumed that the influence of the higher level on the energy distribution at 0.5 Mev could be neglected.

It is interesting to compare these results with the work of Geer *et al.*[3] who made a direct measurement of the $(\alpha_1-\alpha_2)$ angular correlations at E_p equal to 163 and 290 kev. The range of angles studied was confined for tween 130° and 180°, but the measurements made be- angles beyond 170° were affected by the detection of the breakup alphas from the ground state Be^8 as well. Their results at 290 kev are reported to be consistent with a (2+) state in C^{12} with the two lowest values of angular momentum for the outgoing α_1, and also to be in qualitative agreement with a mixture of (2−) and (1−) states, but not consistent with a pure state of (1−), (2−), or (3+) for any values of the parameter B. However, from the α_1 excitation curves[6,11] an estimate of the ratio of intensities of the 0.67- and 1.4-Mev levels at $E_p=290$ kev gives a value of about one-fourth, and it is perhaps not justifiable to interpret their results in terms of a pure state in C^{12}. The fact that they find qualitative agreement for a mixture of (2−) and (1−) states seems reasonable on the picture we ourselves have come to favor.

IV. ELASTIC SCATTERING OF PROTONS

(a) Experimental Method

The differential cross section for the elastic scattering of protons by boron-11 was studied for proton energies E_p between 200 and 900 kev. The apparatus used has already been described,[14] the protons being studied with a rotatable magnetic analyzer of 2% resolution.

The detector in this experiment was a secondary-electron multiplier of 14 stages which counted low-energy protons down to 200 kev with an efficiency greater than 90% at a bias above the region of background pulses. An electromagnetically-separated iso-

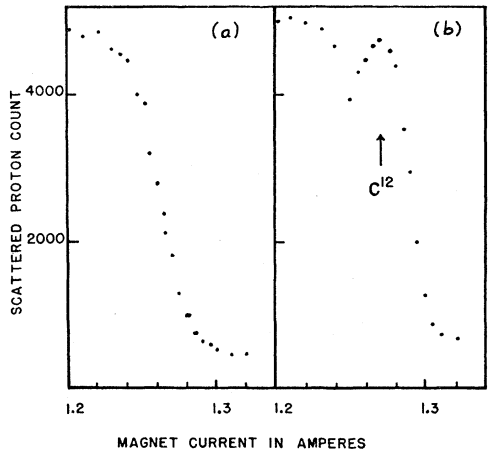

FIG. 5. Profile of the scattered protons from a thick boron target: (a) fresh and (b) with surface contamination of carbon. The proton energy $E_p=0.48$ Mev.

[14] G. Dearnaley, Phil. Mag. 1, 821 (1956).

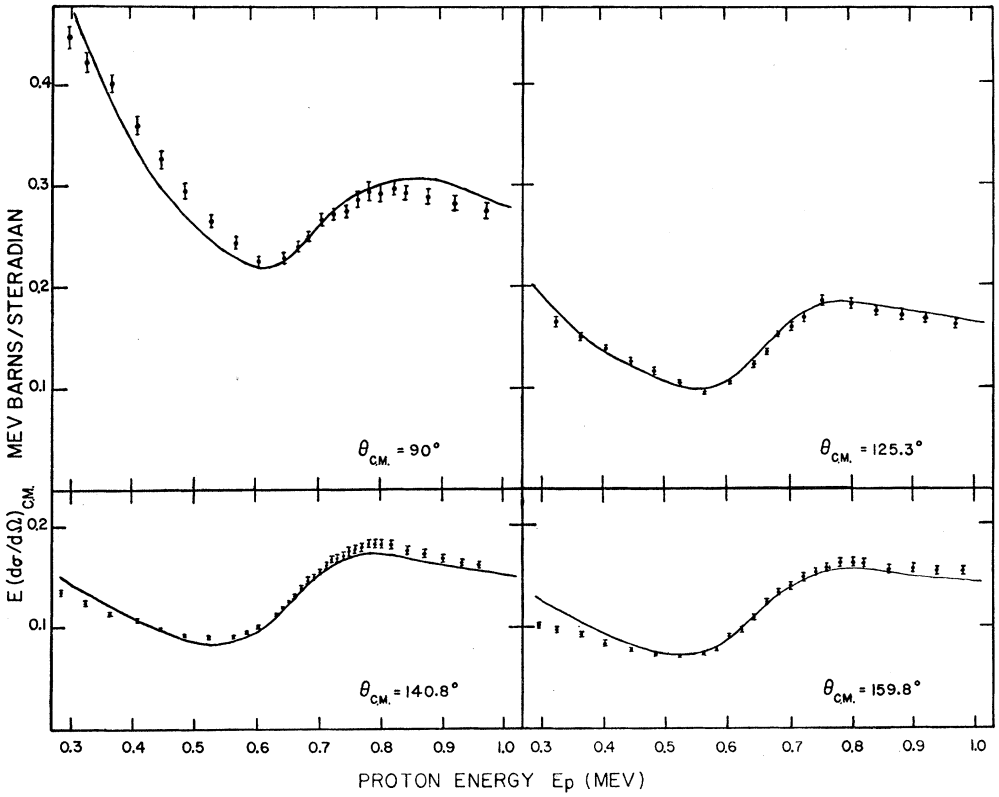

FIG. 6. Variation of the product of the center-of-mass scattering cross section $(d\sigma/d\Omega)_{c.m.}$ and the scattered proton energy E as a function of the incident proton energy E_p. The curves are the theoretical fit to the experimental points for the four scattering angles $\theta_{c.m.}$ equal to 90°, 125.3°, 140.8°, and 159.8°.

topic B^{11} target of thickness 2.7 mg/cm^2 was used; the momentum spectrum of the scattered protons at 0.48 Mev is shown in Fig. 5(a). A study of the accumulation of carbon on the target after a bombardment greatly exceeding that used in the experiment showed that the height of the edge of the proton group scattered off B^{11} was not appreciably affected, and the carbon layer caused only a negligible shift in the energies of protons scattered off boron. This is shown clearly in Fig. 5(b).

In the experiment a current integrator[14] was used to count the scattered protons corresponding to a certain register of charge collected on the target. The edge of the profile of the proton group was studied at small energy intervals for four scattering angles, $\theta_{c.m.}$ in the center-of-mass system, equal to 90°, 125.3°, 140.8°, and 159.8°, for which the lower order Legendre polynomials have zeros.

(b) Results and Analysis

The yield of the scattered protons was measured at the edge of the profile so the energy E of the scattered particles is related to the incident energy E_p by $E=E_p(M^2+1+2M\cos\theta_{c.m.})/(M+1)^2$, where M is the atomic weight of the target nucleus. The differential cross section $(d\sigma/d\Omega)_{c.m.}$ in the center-of-mass system was determined from the yield after correcting for the spread in energy of particles accepted by the magnet analyzer and the stopping power of the target material (which is a known function of the energy E) and finally converting the cross-section values to the center-of-mass system. The product $E(d\sigma/d\Omega)_{c.m.}$ has been plotted in Fig. 6 as a function of the proton energy E_p for the four scattering angles. The absolute cross-section values given as ordinates were obtained by a comparison of the scattered proton yield from boron-11 with that from a copper target, assuming the latter scattering to be of the simple Rutherford type. The relative accuracy or spread of the experimental points is around 3%, and is due to the statistical error in the proton count and the inaccuracies involved in the current-integrator measurements, in the calculation of the stopping power, and in the subtraction of the background due to impurities in the target. The absolute cross-section values given are probably accurate to 10%.

The curves have been fitted by a graphical method of analysis[15] in which the coherent scattering amplitudes and phases are represented by vectors in the complex plane, and the resultant found. The theory of elastic scattering and the formulas for the vectors have been worked out,[16] and have already been detailed in the previous paper by Dearnaley.[14]

In the energy region studied, the two resonances at 0.67- and 1.4-Mev proton energy would influence the

[15] R. A. Laubenstein and M. J. W. Laubenstein, Phys. Rev. 84, 18 (1951).
[16] J. M. Blatt and L. C. Biedenharn, Revs. Modern Phys. 24, 258 (1952).

scattering; the widths Γ of the levels have been given as 330 kev and 1.27 Mev, respectively.[6] The partial proton widths Γ_p of these levels are not accurately known and have been taken as adjustable parameters in the analysis. The hard-sphere corrections were made assuming a nuclear radius of 3.34×10^{-13} cm, but the calculations are not very sensitive to this choice.

One important conclusion stands out from the experimental results of Fig. 6. It is seen that the scattering anomaly is pronounced at all angles including 90°, which strongly suggests that the angular momentum of the incident protons producing the resonance at 0.67 Mev must be zero. P-wave scattering would give no coherent effect at 90°, since the greatest contribution to the anomaly, the interference between nuclear and Coulomb scattering, varies as $P_l(\cos\theta)$ and, for $l=1$, would be zero at this angle. Higher angular momenta for the protons forming the resonance state are similarly excluded, and would not in any case be favored in this reaction. With the assumption, then, that the two resonances at 0.67 and 1.4 Mev are (2−) and (1−) respectively, and are formed by s-waves only, best agreement is obtained for values of Γ_p/Γ equal to 0.5 for the lower and 0.05 for the higher resonance. A background scattering effect probably due to the influence of broad resonances at still higher energies was found in the results and an empirical vector of constant amplitude and phase has been assumed to take account of this. The vector diagram as used at the resonance energy 0.67 Mev and for $\theta_{c.m.}=90°$ is shown in Fig. 7. The theoretical curves drawn in Fig. 6 on the above assumptions seem in good agreement with experiment considering the fact that a possible variation of the background scattering effect with energy has not been taken into account; this background appears to be decreasing at lower proton energies as might be expected. The slight broadening and the shift of the anomaly to lower energies for larger scattering angles is faithfully reproduced. It should be noted here that if a mixture of both s- and d-waves is assumed for the ingoing protons forming the 0.67-Mev resonance, the scattering results would exclude a d-wave amplitude contribution of more than 10% of the total.

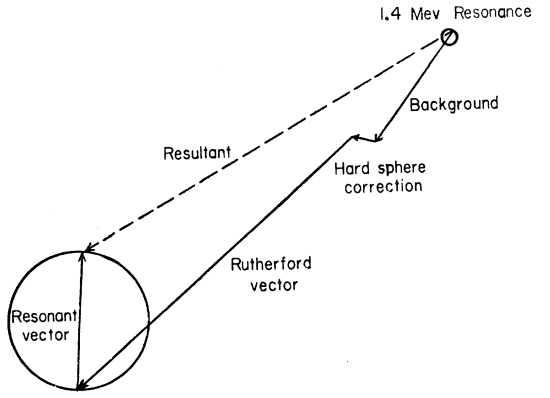

FIG. 7. Vector diagram used to obtain the scattering cross section, drawn for $E_p=675$ kev and $\theta_{c.m.}=90°$. The circle is the locus of the end point of the resonant vector.

V. SUMMARY AND DISCUSSION

The results of our study of several reactions involving the states in C^{12} at 0.67- and 1.4-Mev proton energy give a consistent picture of the properties of these states. Perhaps the best evidence for the character of the 0.67-Mev state comes from our data on the elastic scattering of protons by boron-11 where the presence of an anomaly at a scattering angle of 90° excludes the formation of this state by p-wave protons, and therefore rules out an assignment (2+) to the state. The energy and angular dependence of the scattering cross sections between 300 and 900 kev fits in well with assignments of (2−) and (1−) respectively for the 0.67- and 1.4-Mev states, with the assumption that these states are formed mainly by s-waves; the d-wave contribution in amplitude to the formation of the lower state is estimated as less than 10%. The scattering data, further, give values for Γ_p/Γ as 0.5 for the lower and 0.05 for the higher state. This value of Γ_p for the 1.4-Mev state agrees with one of the alternatives suggested by our experiments[5] on the (p,α_0) and (p,α_1) yields, and is also in accord with the recent results on the (p,p) scattering measured at one angle by Tautfest and Rubin[17] that indicated a narrow proton width to the state. The Γ_p value of 0.5 for the 0.67-Mev state agrees with that of Beckman *et al.*[1]

The (p,α_0) angular distributions for E_p up to 2 Mev show strong interference effects between the 1.4-Mev state and one or more broad states of opposite parity at higher energies. When one uses the known data[9,11] on the relative intensities and widths of the resonances concerned, at 1.4, 2.0, and 2.6 Mev, respectively, the results for E_p below 1.4 Mev are well explained as due to a (1−) state at 1.4 Mev, formed by s- and d-wave protons, influenced mainly by the (2+) broad state resonant at 2.6 Mev, formed by p-wave protons only. In contrast, the (p,α_1) angular distributions up to 1.4 Mev do not give any definite evidence of interference between the 0.67- and 1.4-Mev states, although it must be noted that the method of measurement is somewhat insensitive to the odd powers of $\cos\theta$ in the distribution. The isotropic form of the distributions below about 1 Mev confirms the result from the elastic proton scattering measurements discussed above, that the 0.67-Mev state is formed principally by s-wave protons. The $\cos^2\theta$ term in the α_1 distribution at 1.4 Mev may be explained qualitatively as due to an admixture of both s- and d-wave protons in the formation of this higher state.

The energy distribution of the α_2 particles observed at 90° to the protons of energy $E_p=0.53$ Mev is explained satisfactorily assuming the formation of the

[17] G. W. Tautfest and S. Rubin, Phys. Rev. **103**, 196 (1956).

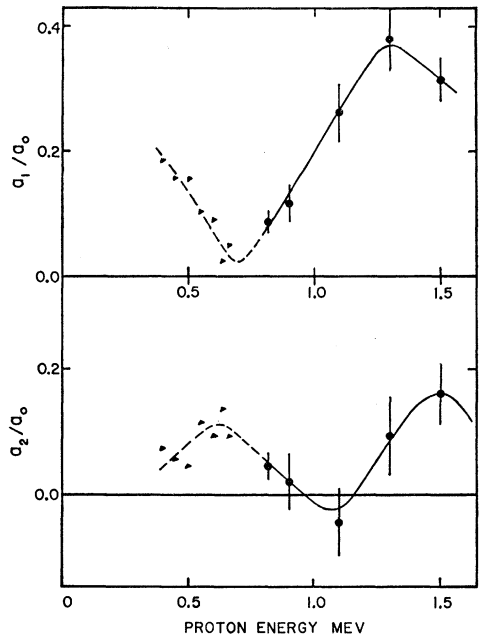

FIG. 8. The results of Gove and Paul (1955) and of Grant *et al.* (1954) on the angular distribution of the 12-Mev gamma rays in $B^{11}(p,\gamma_1)C^{12*}$. The graphs show the variation with incident proton energy of the coefficients a_1/a_0 and a_2/a_0 of the Legendre polynomial expansion of the angular distribution $W(\theta)=P_0+(a_1/a_0)P_1+(a_2/a_0)P_2$, of this gamma ray. It is seen that a single curve can be drawn in each graph through the two sets of results.

0.67-Mev state by s-wave protons, if the state is assigned as (2−), with both p- and f-wave α_1-particles emitted, but not if it is (1−) for any admixture of p- or f-wave α_1 emitted.

Finally we would like to refer to the assignment of (2+) to the 0.67-Mev resonance suggested by Grant *et al.*[8] based on their measurements of the angular distribution of the 12-Mev γ rays in the reaction $B^{11}(p,\gamma_1)C^{12*}$. Gove and Paul[2] have extended these measurements to higher proton energies, and we reproduce in Fig. 8 their values for the coefficients a_1/a_0 and a_2/a_0 for proton energies below about 1.5 Mev. [These coefficients correspond to the Legendre polynomial expansion of the angular distribution of this gamma ray, $W(\theta)=P_0+(a_1/a_0)P_1+(a_2/a_0)P_2$.] Gove and Paul interpreted their measurements as consistent with an assignment of (2−) or (3+) to the 0.67-Mev state, with the former assignment preferred on account of the gamma-ray transition probabilities. We have also plotted in Fig. 8 the values of these coefficients a_1/a_0 and a_2/a_0 as obtained from the results of Grant *et al.*,[8] and it is seen that their values merge well into the curves of Gove and Paul. The minimum in the values of a_1/a_0 (and therefore of the $\cos\theta$ term in the angular distribution) at a proton energy near 700 kev could be readily understood in terms of an interference of the prominent 0.67-Mev state with a broad state which is resonant at some higher energy and whose intensity in the region around 700 kev is comparatively small and slowly varying. This broad state could just as well be the even-parity states at 2.0 and 2.6 Mev as the state at 1.4 Mev, and we do not feel that these results of the angular distribution of the 12-Mev gamma rays conflict in any way with the assignments that are strongly favored by our several studies, namely a (2−) to the 0.67-Mev state and a (1−) to the 1.4-Mev state in C^{12}.

ACKNOWLEDGMENTS

The authors are indebted to Mr. R. H. Lamb for the construction of the secondary-electron multiplier used in the scattering measurements. One of us (G. D.) is grateful for a Senior Research award from the Department of Scientific and Industrial Research, another (G. L. J.) for a research grant from King's College, Cambridge, and a third (G. A. D.) to the Government of Ceylon for the award of a University Scholarship.

APPENDIX. ENERGY DISTRIBUTION OF α_2 WHEN COSγ IS NEAR ZERO

In the theoretical considerations of Sec. III (a) for determining the energy distribution of the α_2 particles in the reaction $B^{11}(p,\alpha_1)Be^{8*}\rightarrow 2\alpha_2$, we assumed that the solid angle available to particles in the third stage of the process was given by $A_0/v_3^2\cos\gamma$, where A_0 is the area $(=V^2\delta\omega)$ subtended at C by a cone of solid angle

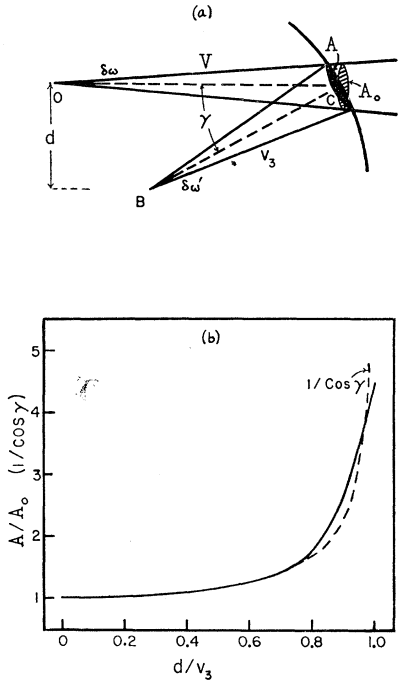

FIG. 9. (a) The solid angle $\delta\omega'$ available to the α_2-particles as defined by the area of intersection A of a cone, of solid angle $\delta\omega$ and axial length V, and a sphere with center B and radius v_3. The area A_0 is equal to $V^2\delta\omega$ and the ratio A/A_0 is assumed equal to $1/\cos\gamma$ in the simplified treatment of Sec. III. (b) The plot of A/A_0 against d/v_3 (i.e. $\sin\gamma$), as obtained empirically, is shown in the smooth curve, the variation of $1/\cos\gamma$ in the broken curve.

$\delta\omega$ and apex 0 [as shown in Fig. 9(a)]. This assumption is not valid for cosγ near or equal to zero. The correct solid angle $\delta\omega'$ available in the third stage is A/v_3^2 so that the ratio A/A_0 should correspond to $1/\cos\gamma$ in the simplified treatment of Sec. III. The value for dn for the general case [see Eq. (2)] should therefore be

$$dn=N\delta\omega\,\sin\rho d\rho(V^2/v_3^2)f(\phi)\int_{\psi=0}^{2\pi}(A/A_0)d\psi. \quad (7)$$

The measurement of A/A_0 was carried out experimentally by using a narrow pencil of divergent light incident on the surface of a large glass globe. The arrangement used simulated the nature of the problem as indicated in Fig. 9(a). With V kept fixed throughout, the area A of the spot of light was measured as a function of the depth d of B below the axis of the cone of light. There would, in fact, be two spots of light corresponding to angles γ and $\pi-\gamma$. The measurements were made on the spot nearer the source, i.e., for $\pi/2\leqslant\gamma\leqslant\pi$; since the distance V to the spot of light was kept constant the variation of the area of the spot for $\pi/2\geqslant\gamma\geqslant 0$ would be the same as in the region measured. So long as the axis of the cone of light intersected the sphere in two points, it was possible to identify the two spots separately and to measure the area of one of them; when the axis of cone just touched the sphere, i.e., when $\cos\gamma=0$ or $d=v_3$, the spots merged into one, and in this case the total area was measured. The area A_0 corresponded to the case in which $d=0$. In Fig. 9(b) the measured ratio A/A_0 is valid except for d/v_3 near 1. The quantity d/v_3 (or $\sin\gamma$) is related to the angle ψ (see Fig. 2) in the form

$$b\cos\psi=a-[1-(d/v_3)^2]^{\frac{1}{2}}, \quad (8)$$

where a and b are defined as before in Sec. III (a), and given by

$$a=\cos\epsilon\cos(\phi-\rho)=(E_3+E_1+E-E_2)E^{\frac{1}{2}}/2(E+E_1)E_3^{\frac{1}{2}},$$
$$b=\sin\epsilon\sin(\phi-\rho).$$

With values of E_2, E_3, and E_1 kept fixed, we can use Eq. (8) to determine the variation of d/v_3 for different E as ψ varies from 0 to 2π. The corresponding values of A/A_0 can then be plotted as a function of ψ, as shown in Fig. 10(a) for the particular case when $E_1=0.015$ Mev, $E_2=1.46$ Mev, $E_3=0.15$ Mev, with values of E ranging from 1.0 to 2.5 Mev. The area Y under each curve of Fig. 10(a) gives a value proportional to the integrand

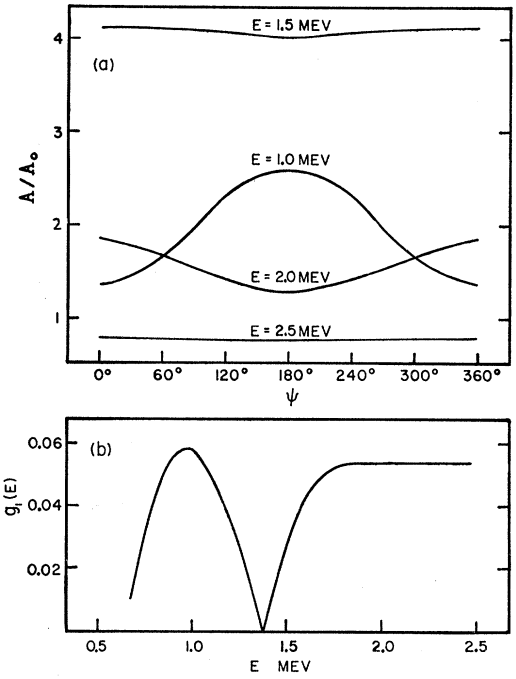

FIG. 10. (a) The ratio A/A_0 plotted as a function of ψ for different values of E ranging between 1.0 and 2.5 Mev in the particular case where $E_1=0.015$ Mev, $E_2=1.46$ Mev and $E_3=0.15$ Mev. (b) The energy distribution function $g_1(E)$ [for $f(\phi)=1/4\pi$] plotted as a function of E for the case represented by the curves of (a) above.

of Eq. (7). Substituting for $\sin\rho d\rho$ in terms of E, E_1, E_2, and E_3 and introducing the energy distribution function $g(E)\equiv dn/dE$ as in Eq. (4), we have

$$g(E)\propto E(E+E_1-E_2+E_3)Yf(\phi)/(E+E_1)^{\frac{3}{2}}. \quad (9)$$

As discussed in Sec. III, most energy distributions corresponding to different patterns $f(\phi)$ can be expressed in terms of $g_1(E)$ and $g_2(E)$ corresponding to $f(\phi)=1/4\pi$ and $f(\phi)=(3/8\pi)\sin^2\phi$ respectively. Thus, using the values of $g_1(E)$ and $g_2(E)$ calculated numerically from Eq. (4) for E in the region where the approximate treatment of Sec. III is valid, the corresponding values in the "anomalous" region ($\cos\gamma\simeq 0$) can be deduced by following the variation given in expression (9). As an example, Fig. 10(b) shows $g_1(E)$ plotted as a function of E for the case represented by the curves of Fig. 10(a); it is seen that $g_1(E)$ drops rapidly in the region where cosγ is near zero.